CHEMISTRY
A European Journal

A Journal of
ChemPubSoc Europe

Accepted Article

Title: Boroquinol Complexes with fused Extended Aromatic Backbones - Synthesis and Optical Properties

Authors: Michael Mastalerz, Sven Elbert, Frank Rominger, Philippe Wagner, and Thines Kanagasundaram

To be cited as: *Chem. Eur. J.* 10.1002/chem.201604421

Link to VoR: http://dx.doi.org/10.1002/chem.201604421

Supported by
ACES

WILEY-VCH

10.1002/chem.201604421

WILEY-VCH

FULL PAPER

Boroquinol Complexes with fused Extended Aromatic Backbones – Synthesis and Optical Properties

Sven M. Elbert,[a] Philippe Wagner,[a] Thines Kanagasundaram,[a] Frank Rominger[a] and Michael Mastalerz*[a]

Abstract: Boron-based dyes are attractive synthetic targets due to their large variability of absorption and emission wavelengths. By Pictet-Spengler-cyclizations, followed by oxidation π-extended boroquinol have been synthesized. During optimization of the reaction conditions an unusual dearylation has been found and mechanistically investigated. For two of the synthesized boroquinols, mechanochromic effects with bathochromic shifts up to 50 nm were found upon grinding.

Introduction

Among fluorescent dyes, those based on boron organic complexes moved more and more into the focus of research because of their facile synthetic accessibility, high quantum yields (*Φ*) in different media and chemical and light stability.[1] Within this class, boron-dipyrromethenes (BODIPYs, Figure 1)[1] are one of the most popular and most investigated families.[1c, 2] The optical properties of BODIPYs can be modified by attaching various substituents at the conjugated backbone.[1a, 3] A large variety of BODIPY derivatives[4] and related systems with *N*,*N*-,[1e, 5] *O*,*O*-,[6] and *N*,*O*-chelating[1e, 7] bidentate ligands for four-coordinate fluorescent boron complexes have been introduced and broadened the potential fields of application. Due to the ease of preparation and their excellent optical properties, boranils (Figure 1) with bidentate *N*,*O*-chelating ligands stand out of this vast amount of different groups.[8] The core structure was first described in 1969[9] and its emitting properties were already mentioned in 1973 by Hohaus and co-workers, who described it as a compound with blue fluorescence.[10] In 2011, Ziessel and co-workers rediscovered the boranils and synthesized a number of derivatives.[11] They obtained highly fluorescent complexes (*Φ* up to 90%) and reported about post-functionalizations by palladium-catalyzed cross-coupling reactions. The ease of their synthesis and their good optical properties make boranils interesting alternatives to BODIPY dyes.

It is known for BODIPYs that the emission properties, such as the HOMO-LUMO energy gap, can be fine-tuned not only by substituents,[1a] but also by extension of the π-system through additional fused aromatic rings.[3a] This bears the advantage that in contrast to tuning the emission with substituents with rotational freedom, the rigidity of the system is retained, resulting usually in higher quantum yields.

Formally, boroquinols are fused π-extended boranils (Figure 1).[7b] Boroquinols show large Stokes shifts (>5000 cm^{-1}),[7b, 12] which are desirable due to the decreased reabsorption of the emitted light and are not common for BODIPYs which usually have Stokes shifts around 500 cm^{-1}. They are also emissive in the solid state, which is advantageous for applications as electroluminescent materials.[13]

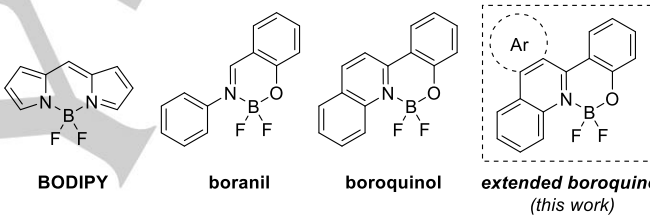

Figure 1. Core structures of selected BF_2-complexes and the target structures of this work.

Most interestingly, only a few boroquinol-derivatives have been published to date.[7b, 14] Donor-acceptor type fused boroquinols have shown emissions with *λ*>600 nm, and theoretical calculations have suggested that they have potential application as n-type semiconductors.[15] In 2012, a series of boroquinol complexes was reported with different substituents on both, the phenolic and the quinolic backbone. These complexes showed excellent quantum yields (*Φ* up to 86%) and a remarkable solvochromic behavior.[12]

Here we describe the synthesis of extended boroquinol analogues (Figure 1) with even larger π-systems containing three or more annulated aromatic rings such as phenanthridines, thioquinolines and benzothienoquinolines by a one-pot Pictet-Spengler-cyclization[16] as a key step for the formation of the *N*,*O*-ligand.

Results and Discussion

Synthesis and Characterization

In 2009, the utilization of the Pictet-Spengler reaction in the synthesis of phenanthridines was described. The reaction occurred under harsh conditions (TFA, 120-140 °C, 1.5 - 7 days), giving the products in isolated yields between 20% and 91%.[17]

[a] S. M. Elbert, P. Wagner, T. Kanagasundaram, Dr. F. Rominger, Prof. Dr. M. Mastalerz
Organisch-Chemisches Institut
Ruprecht-Karls-Universität Heidelberg
Im Neuenheimer Feld 273, 69120 Heidelberg, Germany
E-mail: michael.mastalerz@oci.uni-heidelberg.de

Supporting information for this article is given via a link at the end of the document.

10.1002/chem.201604421

Two equivalents of the aldehyde have been used, with one equivalent probably acting as an oxidant. Recently, a number of 2-substituted phenols with thieno-, pyrrolo-, furo- or oxazoloquinoline backbones and *N*,*O*-chelating binding sites have been introduced by Pictet-Spengler reactions and investigated for the selective binding of fluoride and the use as antitubercular compounds.[18] The reaction procedures varied very largely from mild conditions (20 mol% acetic acid, DMF, 60 °C, 16 h) to harsh ones (e.g. 30 mol% copper(II) triflate, 30 mol% 1,10-phenanthroline, nitrobenzene, 200°C) yielding between 40% and 77% of the corresponding compounds. For a twofold Pictet-Spengler cyclization on a pyrrolo-pyrrole-based system, toluene and TFA have been used as solvents.[19] According to this method, we first reacted 2-amino biaryl **1a**[20] and salicylaldehyde **2** to thienoquinoline **4a** (Scheme 1, Table 1, Entry 1) under similar conditions (PhMe, 20% TFA, 100 °C). Besides the desired product **4a** (59%) substantial amounts of dearylated thienoquinoline **6a**[21] (29%) have been formed. Furthermore, by the analysis of the crude reaction mixture with ^{1}H NMR spectroscopy and UPLC-MS phenol **7** has been identified as another by-product. To the best of our knowledge this kind of dearylation has been mentioned for the first time just very recently for a porphyrin system.[22] However, this side reaction has only been described phenomenological and no suggestion for a reaction mechanism has been given. In this context, it is worth mentioning that in a recent contribution for the Pictet-Spengler reaction of 2-amino biaryls with glyoxylic esters a decarboxylated product similar as in our case was found; again the occurrence of this side reaction has been only described phenomenological and no further investigation towards elucidating the mechanism has been discussed.[23] Since the dearylated product has formed in substantial amounts, we were interested in getting a deeper mechanistically understanding of this reaction to optimize the reaction on a rational basis.

We undertook isolated phenanthridine **4a** the same reaction conditions and could not find any dearylated product **6a**, which verifies the suggestion already done by Paolesse et al.[22] that the dearylation has to occur from the saturated Pictet-Spengler intermediate **9** (see Scheme 2). Two plausible reaction pathways from **9** compete with each other. Either an oxidation of dihydrophenanthridine **9** leads to the desired product **4a** or a protonation of **9** to **10** takes place, followed by a tautomerisation of the phenol unit to the keto form **11**, allowing the compound to undergo cleavage of the C-C bond (in principle a retro-Mannich or retro-hetero-ene reaction[24]), resulting in dearylated thienophenantridine **6a**. As a consequence, the presence or absence and type of oxidant as well as the acid concentration should play major roles to shift the reaction outcome either to **4a** or **6a**. Thus we first studied the influence of acid concentration under consistent conditions.

In order to optimize the reaction conditions, the acid concentration and different atmospheres were tested (Table 1).

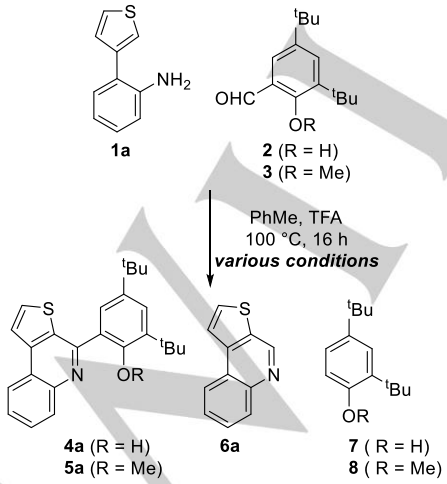

Scheme 1. Reaction of 2-amino biaryl **1a** with aldehydes **2** or **3** under various conditions (see Table 1).

Table 1. Optimization of the reaction condition of the Pictet-Spengler reaction of biaryl **1a** and aldehydes **2** or **3**.

Entry	RCHO (equiv.)	Atm	PhMe:TFA[a]	Yield [%][b]		
				4a/5a	**6a**	**7/8**[c]
1	**2** (1.0)	Air	80:20	59 (**4a**)	29	8 (**7**)
2	**2** (1.0)	Air	90:10	66 (**4a**)	13	10 (**7**)
3	**2** (1.0)	Air	95:05	55 (**4a**)	9	7 (**7**)
4	**2** (1.0)	Air	99:01	25 (**4a**)	n.d.[d]	n.d. (**7**)
5	**2** (1.0)	Ar	50:50	18 (**4a**)	67	n.d. (**7**)
6	**2** (1.0)	Ar	80:20	18 (**4a**)	68	22 (**7**)
7	**2** (1.0)	Ar	90:10	31 (**4a**)	26	25 (**7**)
8	**2** (1.0)	Ar	95:05	46 (**4a**)	12	11 (**7**)
9	**2** (1.0)	Ar	99:01	21 (**4a**)	5	5 (**7**)
10	**3** (1.0)	Air	90:10	66 (**4a**)	n.d.	n.d. (**8**)
11	**2** (2.0)	Air	90:10	75 (**4a**)	17	12 (**7**)
12	**3** (2.0)	Air	90:10	86 (**4a**)	n.d.	n.d. (**8**)
13	**2** (1.0)	O_2	90:10	84 (**4a**)	n.d.	n.d. (**8**)

[a] v/v. [b] Determined by ^{1}H NMR spectroscopy, using mesitylene as internal standard. [c] Note that **7** and **8** are volatile compounds and might be partially lost during work up. [d] n.d.: not detected.

Under ambient atmosphere the conversions were between 55% and 75% with increasing amount of dearylation at higher acid concentrations (Entries 2-4). Lower acid concentration diminished the amount of dearylation product **6a**, but also the formation of desired phenanthridine **4a**. An acid concentration of 1% led to low conversions to **4a** (25%, Entry 4 in Table 1). To suppress the possibility for the oxidation pathway, the reactions were performed under various acid concentrations in argon

10.1002/chem.201604421

atmosphere (Entries 5-9). With acid concentrations as high as 50 vol% the dearylated product **6a** becomes the main product, formed in 67% besides 18% of **4a** (Entry 5). With decreasing amount of acid, the amount of dearylation product **6a** decreases and the ratio of **6a**/**4a** switches towards **4a** with a maximum at a 5% acid concentration

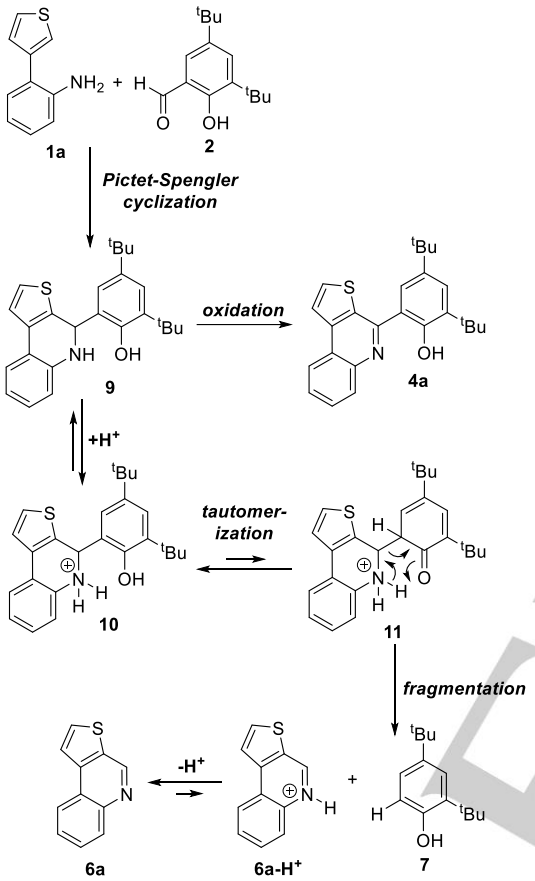

Scheme 2. Two possible pathways from intermediate **9**. Pathway 1: Oxidation to thienoquinoline **4a**. Pathway 2: Proton catalyzed dearylation to thienoquinoline **6a** and phenol **7**.

(Entry 8). With only 1 vol% of acid (Entry 9), both products **4a** and **6a** are generated in lower amounts, similar to the reaction done in air (Entry 4). This clearly demonstrates that the reaction pathway to the desired product **4a** is driven by the oxidant, and the one to the dearylation product by the amount of acid. To prove the tautomerization and C-C-cleavage steps, salicyl aldehyde ether **3** has been synthesized[25] (see Supporting Information) and used in the reaction with biaryl **1a** under the same conditions as the free phenol (10 % TFA, air; Entry 10). As expected, no formation of dearylated product could be observed, due to the fact that a Pictet-Spengler intermediate with a phenol ether cannot undergo no tautomerization and only the corresponding phenanthridine **5a** was detected to be formed in 66%. As mentioned before, the original procedure of Youn et al. used 2.0 equivalents of aldehyde, most likely because one equivalent is acting as oxidant. Therefore, the so-far best conditions (10 vol% TFA, air), have been used for reactions with two equivalents of both, **4a** and **5a** (Entries 11-12) to elevate the product formation to 75% (**4a**) or 86% (**5a**). From an atom-economically point of view, it is not ideal to sacrifice half of the salicylaldehyde as oxidant. Therefore, the 1:1-stoichiometric reaction of **1a** and **2** was finally performed with molecular oxygen as oxidant in toluene (with 10 vol% TFA) at 100 °C, giving 91% of the desired product **4a** and only traces of dearylation products **6a** and **7** (Entry 13).

After the successful elucidation of suitable reaction conditions, a series of π-extended compounds was synthesized. Suzuki-Miyaura cross-coupling reactions[26] of boronic acids **12a-d**[27] with bromoaniline **13** afforded the required 2-aminobiaryls **1a-d**[20, 28] in 48-95% yield (Scheme 3 and Table 2). Biaryls **1a-d** were then reacted with aldehydes **2** or **3** under the optimized reaction conditions (PhMe, TFA, O_2, 100 °C), giving the ligands **4a-d** in 52-76% isolated yield. Reactions under ambient atmosphere showed the discussed dearylation for all systems with isolated yields of **6a-d**[21, 29] of 15-17% and lower yields of the desired ligands **4a-d** in comparison to the optimized conditions (Scheme 3 and Table 2).

For a detailed spectroscopical analysis of the final BF_2-complexes (**14a-d**) the phenol ethers **5a-5d** were synthesized under the same conditions in 54-84% isolated yields.

4a-d were treated with borontrifluoride etherate ($BF_3{\cdot}Et_2O$) and triethylamine to give the BF_2-complexes **14a-d** in 32-84% yield (Scheme 3 and Table 2). It was found that complex **14d** with two methoxy groups is decomposing in solution with time, which probably is the reason for the lower yield in this case.

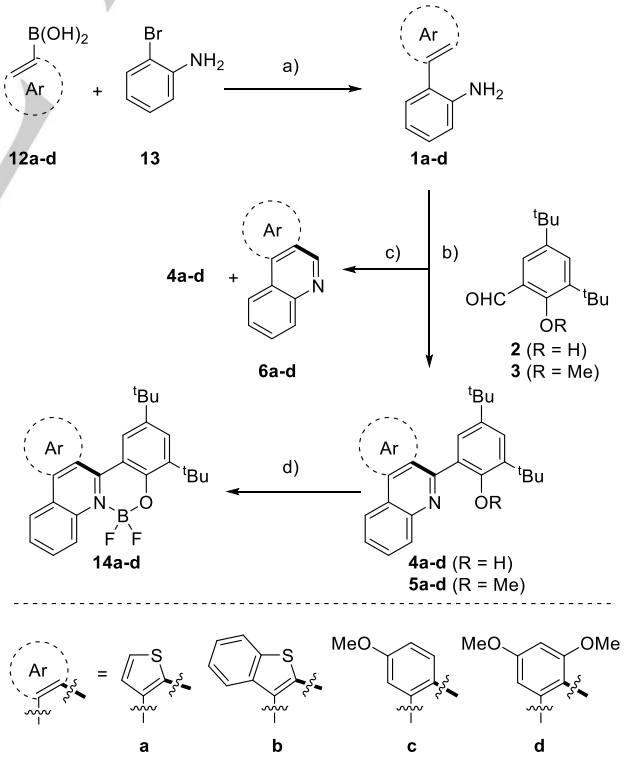

Scheme 3. Synthesis of complexes **14a-d**. Reagents and conditions: a) Pd_2dba_3, $HP^tBu_3BF_4$, THF, $K_2CO_{3\,(aq.)}$ (1 M), 80 °C, 16 h; b) **2** or **3**, PhMe, TFA, O_2, 100 °C, 16 h; c) **2,** PhMe, TFA, air, 100 °C, 16 h; d) R=H, $BF_3{\cdot}Et_2O$, Et_3N, CH_2Cl_2, r.t., 16 h. For isolated yields see Table 2.

10.1002/chem.201604421

FULL PAPER

Table 2. Isolated yields of the cross-coupling, cyclization and complexation reactions towards complexes **14a-d** as depicted in Scheme 3.

Entry	Ar	Yield of [%]				
		1	**4**	**6**	**5**	**14**
1	**a**	73 (**1a**)	74[a]/42[b] (**4a**)	0[a]/15[b] (**6a**)	78 (**5a**)	84 (**14a**)
2	**b**	48 (**1b**)	52[a]/46[b] (**4b**)	0[a]/17[b] (**6b**)	54 (**5b**)	80 (**14b**)
3	**c**	95 (**1c**)	60[a]/35[b (**4c**)	0[a]/16[b] (**6c**)	66 (**5c**)	68 (**14c**)
4	**d**	80 (**1d**)	76[a]/56[b (**4d**)	0[a]/15[b (**6d**)	84 (**5d**)	32 (**14d**)

[a] Oxygen atmosphere. [b] Ambient atmosphere.

With the optimized procedure, a system with five annulated rings and two *N*,*O*-chelating moieties was accessible (Scheme 4): Phenylenediamine **15** was synthesized by Suzuki-Miyaura cross-coupling (see Supporting Information) and subsequently reacted with aldehydes **2** or **3** under the mentioned optimized conditions (PhMe, TFA, O_2) to afford **17** in 46% yield. In contrast, methyl protected derivative **16** could be synthesized in higher yields of 76%. The ether functions in **16** can also be cleaved with BBr_3 giving **17** in 72%, thus the combined yield for this two-step approach is slightly higher with 54%. Ligand **17** was converted to BF_2-complex **18** with borontrifluoride etherate and di-isopropylamine in 70% yield.

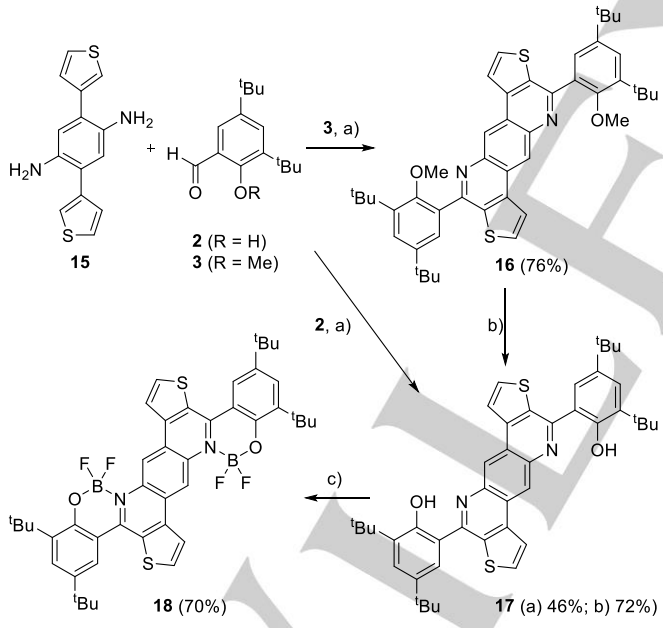

Scheme 4. Synthesis of complex **18**. Reagents and conditions: a) PhMe, TFA, O_2, 100 °C, 3 h; b) BBr_3, CH_2Cl_2, 0 °C-r.t., 20 h; c) $BF_3{\cdot}Et_2O$, $^iPr_2NH$, $C_2H_4Cl_2$, 85 °C, 16 h.

A comparison of ^{1}H NMR spectra of compounds with the same aromatic backbones (here thienoquinolines **5a**, **4a** and **14a**, Figure 2 and Table 3) allows first insights on intramolecular interactions. **5a** shows no hints of coplanarity of its aromatic systems in solution on the NMR time-scale. The planarity is increased through the formation of a hydrogen bond between the hydroxyl proton and the nitrogen in ligand **4a** leading to a pronounced downfield shift of proton H^h of $\Delta\delta$ = +0.8 ppm from **5a** (δ = 7.45 ppm) to **4a** (δ = 8.26 ppm), which can be explained by a resulting intramolecular C-H···S contact of proton H^h.[30] In complex **14a** no rotational freedom along the biaryl axis is possible and consequently this intramolecular interaction is evidenced by a negligible change of the chemical shift of proton H^h in **14a** (δ = 8.17 ppm) compared to **4a** (δ = 8.26 ppm). In addition, an intramolecular hydrogen bond (C-H···F interaction) between H^f and one fluorine of the BF_2-moiety of **14a** is apparent by a significant downfield shift of proton H^f in complex **14a** (δ = 8.91 ppm) compared to **5a** (δ = 8.32-8.35 ppm) or **4a** (δ = 8.20 ppm).[31] The interaction to a single fluorine atom is furthermore supported by the presence of two signals in the corresponding ^{19}F NMR spectrum (δ = -140.6 ppm and δ = -140.5 ppm for complex **14a**) with a coupling of the fluorine to the carbon bound proton H^f (δ = 125.4 ppm, J = 8.1 Hz) "through space".[32] The C-H···S interactions can be also found for the benzothienoquinoline ligand **4b** and complex **14b** as well as for the extended systems **17** and **18** (for chemical shifts see Table 3) and the C-H···F hydrogen bond are observed for all complexes **14a-d** and **18**, but will not be discussed here in detail (chemical shifts of corresponding protons and carbons in Table 3). Interestingly, all these interactions are found also in the solid state (see discussion below).

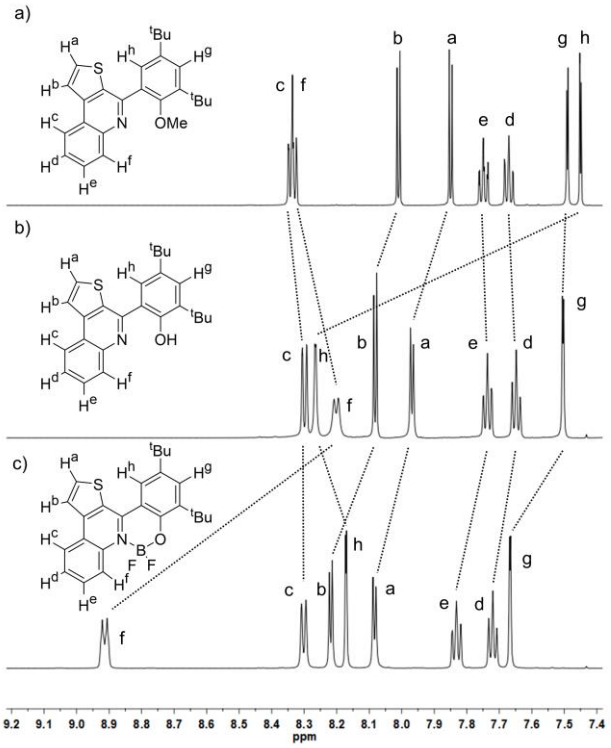

Figure 2. Comparison of ^{1}H NMR spectra of: a) **5a**; b) **4a**; c) **14a** in $CDCl_3$ at 600 MHz and room temperature with signal assignment.

10.1002/chem.201604421
WILEY-VCH

FULL PAPER

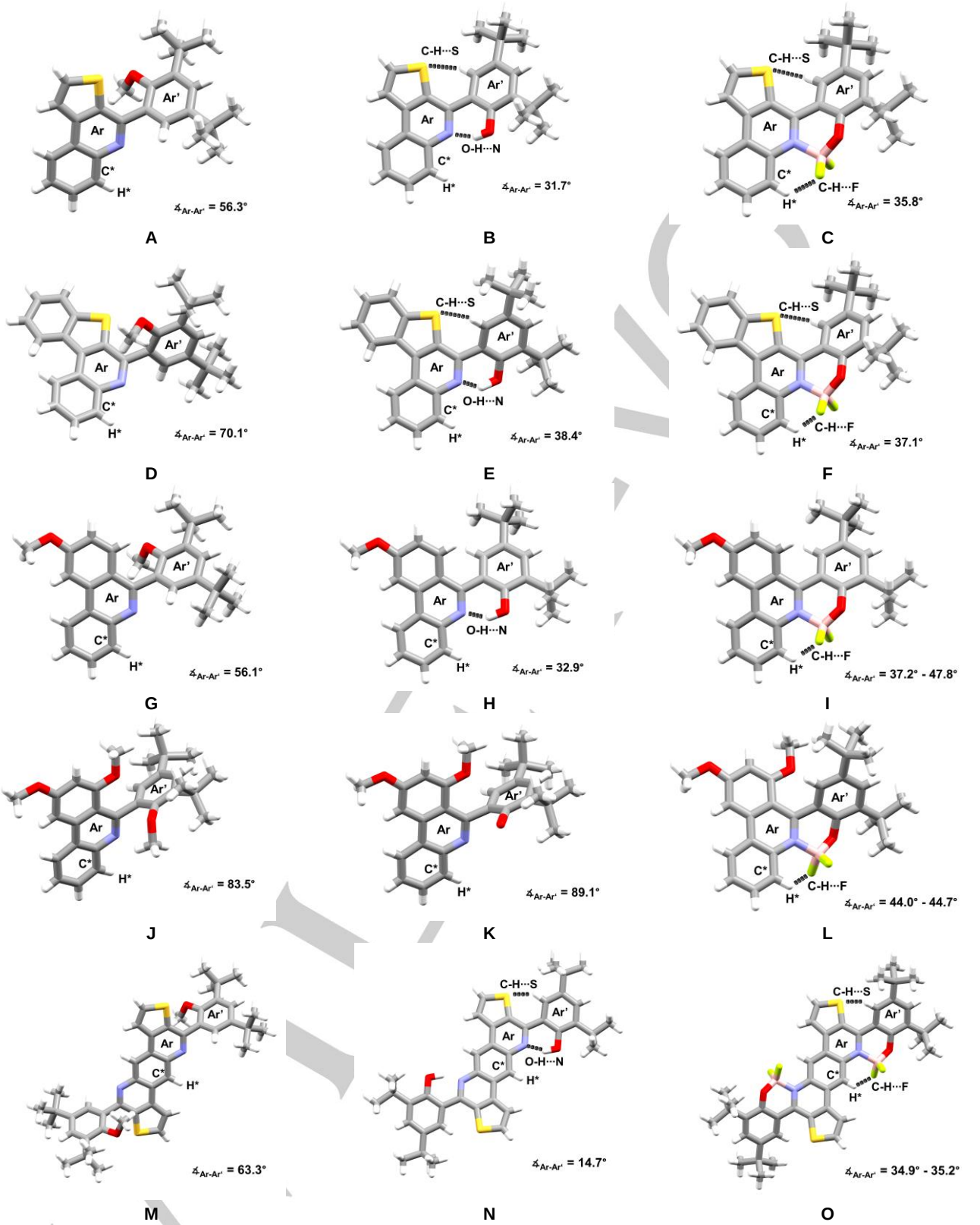

Figure 3. Capped sticks representations of crystal structures of molecules **5a, 4a** and **14a** (A-C), molecules **5b, 4b** and **14b** (D-F), molecules **5c, 4c** and **14c** (G-I), molecules **5d, 4d** and **14d** (J-L) and molecules **16-18** (M-O). The given angles are measured as angle between mean planes of the aromatic systems Ar and Ar'. The chemical shifts of carbon C* and proton H* and the lengths of the intramolecular C-H···S, O-H···N and C-H···F contacts can be found in Table 3. Colors: Carbon: grey; Oxygen: red; Nitrogen: blue; Boron: rose; Fluorine: yellow; Hydrogen: white.

10.1002/chem.201604421

FULL PAPER

Table 3. Selected NMR spectroscopic and crystallographic data.

Compound	δ_{H^*}[a] [ppm]	δ_{C^*}[b] [ppm]	$\measuredangle_{Ar\,Ar'}$[c] [°]	$d_{C\text{-}H\cdots S}$ [Å]	$\measuredangle_{C\text{-}H\cdots S}$ [°]	$d_{O\text{-}H\cdots N}$ [Å]	$\measuredangle_{NHO}$ [°]	$d_{B\text{-}N}$ [Å]	$\measuredangle_{NBO}$ [°]	$d_{C\text{-}H\cdots F}$ [Å]	$\measuredangle_{CHF}$ [°]
4a	8.20	128.2 (s)	31.7	2.506	120.0	1.726	154.0	-	-	-	-
4b	8.28-8.25	129.2 (s)	38.4	2.543	115.4	1.612	147.2	-	-	-	-
4c	8.09	126.9 (s)	32.9	-	-	1.687	150.9	-	-	-	-
4d	8.03	129.0 (s)	89.1	-	-	-	-	-	-	-	-
5a	8.35-8.32 (m)	130.2 (s)	56.3	-	-	-	-	-	-	-	-
5b[d]	8.43	131.2 (s)	70.1	-	-	-	-	-	-	-	-
5c	8.25	130.5 (s)	56.1	-	-	-	-	-	-	-	-
5d	8.19	128.8 (s)	83.5	-	-	-	-	-	-	-	-
14a	8.91	125.4 (t)	35.8	2.501	116.1	-	-	1.639	106.4	2.166	119.0
14b	9.02	125.8 (t)	37.1	2.443	-	-	-	1.619	108.7	2.282	112.6
14c[e]	8.82	125.4 (t)	37.2	-	-	-	-	1.618	109.8	2.355	115.7
			37.4	-	-	-	-	1.624	108.9	2.383	111.5
			47.8	-	-	-	-	1.613	109.5	2.332	112.4
14d[e]	8.81	125.0 (m)	44.0	-	-	-	-	1.589	110.3	2.365	109.7
			40.0	-	-	-	-	1.627	108.4	2.214	115.6
			44.7	-	-	-	-	1.618	109.1	2.320	111.0
16	9.32	123.9 (s)	63.3	-	-	-	-	-	-	-	-
17	9.07	122.9 (s)	14.7	2.354	135.9	1.618	151.2	-	-	-	-
18[f]	9.89	120.2 (t)	34.9	2.538	120.6	-	-	1.617	109.7	2.333	109.5
			35.2	2.506	117.3	-	-	1.636	108.6	2.331	111.1

[a] The position of proton H* is depicted in Figure 3. [b] The position of proton C* is depicted in Figure 3. [c] Measured as angle of mean planes of the aromatic systems Ar and Ar' as depicted in Figure 3. [d] A crystal structure was obtained, but can be only seen as proof of constitution due to low quality. [e] Three independent molecules can be found in the crystal structure. [f] Two independent molecules can be found in the crystal structure.

Single Crystal X-Ray Analysis

All compounds have been studied by single-crystal X-ray diffraction analysis.

The comparison of the X-ray crystal structures of **5a**, **4a** and **14a** (Figure 3A-C) supports the conclusion drawn by ^{1}H NMR spectroscopy. Methoxy derivative **5a** shows no intramolecular interactions due to a torsion angle between its aromatic systems Ar and Ar' of $\measuredangle_{Ar\text{-}Ar'}$ = 56.3° (Figure 3B and Table 3). The hydrogen bond (O-H···N) with a length of $d_{O\text{-}H\cdots N}$ = 1.726 Å in ligand **4a** forces the aromatic systems Ar and Ar' to planarize ($\measuredangle_{Ar\text{-}Ar'}$ = 31.7°) and causes the formation of a C-H···S contact with $d_{C\text{-}H\cdots S}$ = 2.506 Å.

A comparable torsion angle ($\measuredangle_{Ar\text{-}Ar'}$ = 35.8°) and C-H···S contact ($d_{C\text{-}H\cdots S}$ = 2.501 Å) can be found in complex **14a** (Figure 3C and Table 3) and additionally a C-H···F contact with $d_{C\text{-}H\cdots F}$ = 2.166 Å as indicated by ^{1}H NMR spectroscopy (the chemical shifts of protons H* and the multiplicity of carbon nuclei C* was discussed before and is summarized in Table 3). Benzothienoderivatives **5b**, **4b** and **14b** as well as methoxyphenanthridines **5c**, **4b** and **14c** show analogous trends as the ones discussed (Table 3).

Only the dimethoxyphenanthridines **5d**, **4d** and **14d** show larger torsion angles (**5d**: $\measuredangle_{Ar\text{-}Ar'}$ = 83.5°; **4d**: $\measuredangle_{Ar\text{-}Ar'}$ = 89.1°) due to sterical hindrance of the methoxygroup in 7-position. Ligand **4d** is therefore the only ligand without an intramolecular hydrogen bond and is forming hydrogen bonded dimers. The smallest torsion between Ar and Ar' was found for extended bis-ligand **17** with $\measuredangle_{Ar\text{-}Ar'}$ = 14.7°.

10.1002/chem.201604421

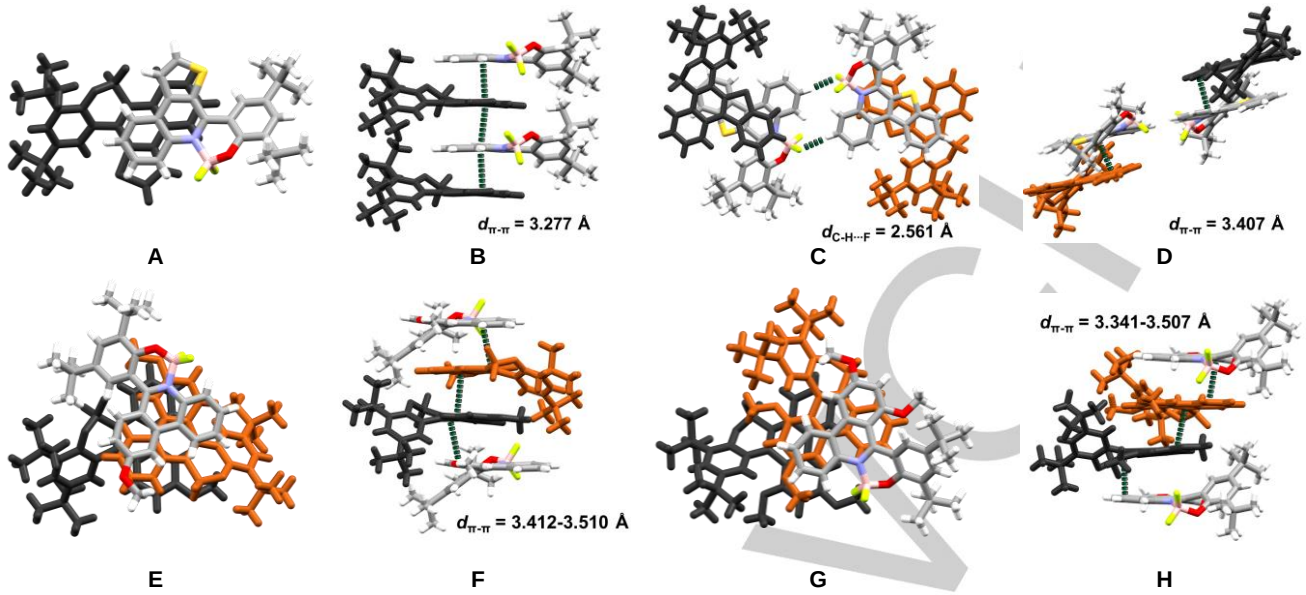

Figure 4. Capped sticks representations of packing motifs in x-ray crystal structures of: Complex **14a** (A and B); Complex **14b** (C and D); Complex **14c** (E and F); Complex **14d** (G and H). C-H···F contacts (C) and π-π interactions (B, D, F, H) are shows as dotted green lines. Colors: Carbon: grey; Oxygen: red; Nitrogen: blue; Boron: rose; Fluorine: yellow; Hydrogen: white.

The observations made by single crystal x-ray analysis on the intramolecular interactions in solid state are in good agreement to the ones in solution made by ^{1}H NMR spectroscopy and seem to be not driven by packing effects.

Complexes **14a-d** all show π-π stacking motifs. Complex **14a** packs in offset columns (Figure 5A and B) with a distance of $d_{\pi\text{-}\pi}$ = 3.277 Å that are aligned through C-H···F and dispersion interactions perpendicular to the direction of the columns. Complex **14b** forms dimers through C-H···F interactions of $d_{C\text{-}H\cdots F}$ = 2.561 Å with an offset π-π stacking of $d_{\pi\text{-}\pi}$ = 3.407 Å (Figure 5C and D). The so created sheets interact with solvent molecules (CH_2Cl_2) through C-H···F and Cl···π interactions. Complexes **14c** and **14d** pack in a comparable way with helical columns of the three independent molecules with π-π interactions of $d_{\pi\text{-}\pi}$ = 3.34-3.51 Å which are aligned through C-H···F and C-H···π and dispersion interactions (Figure 5E, F, G and H).

Complex **18** forms ribbons through intermolecular C-H···F interactions of one fluorine of a BF_2 unit and the proton in α-position to the sulfur atom of the extended backbone with $d_{C\text{-}H\cdots F}$ = 2.399 Å (Figure 5A). These ribbons align in a herringbone like manner via Cl-S, C-H···F and C-H···Cl interaction over solvent molecules ($CHCl_3$) as depicted in Figure 5B.

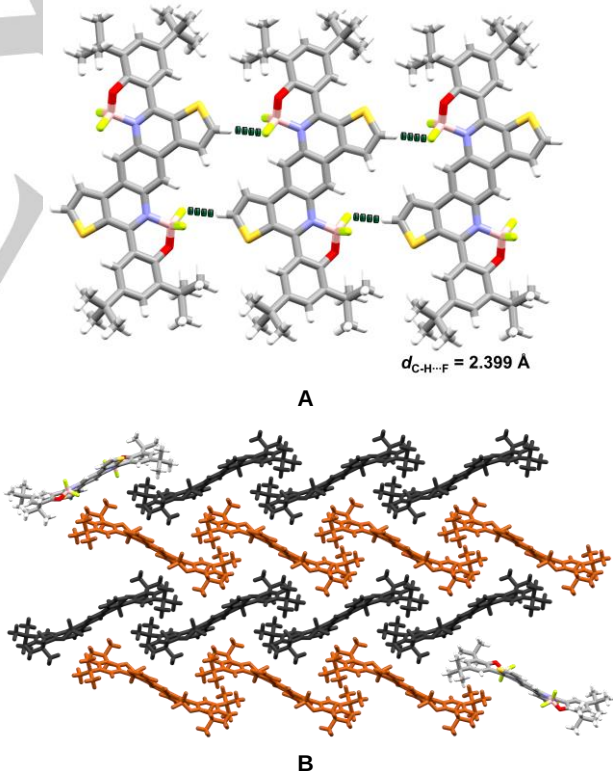

Figure 5. Capped sticks representations of packing motifs in the x-ray crystal structures of complex **18**. The green dotted lines in A illustrate C-H···F contacts. Colors: Carbon: grey; Oxygen: red; Nitrogen: blue; Boron: rose; Fluorine: yellow; Hydrogen: white.

10.1002/chem.201604421

Table 4. Spectroscopic properties.

Compound	Solvent	λ_{abs} (lg ε) [nm][a]	λ_{em} (λ_{ex}) [nm][a]	Stokes Shift [cm^{-1}]	Φ[b]	T [ns]	k_f (10^8 s^{-1})[c]	k_{nr} (10^8 s^{-1})[d]
4a	$CHCl_3$	364 (3.95)	-[e]	-	-	-	-	-
4b	$CHCl_3$	384 (4.02)	-[e]	-	-	-	-	-
4c	$CHCl_3$	359 (3.76)	-[e]	-	-	-	-	-
4d	$CHCl_3$	363 (3.87)	-[e]	-	-	-	-	-
5a	$CHCl_3$	339 (3.86)	-[e]	-	-	-	-	-
5b	$CHCl_3$	366 (3.86)	388 (324)	1549	0.07	0.70	1.00	13.3
5c	$CHCl_3$	346 (2.84)	-[e]	-	-	-	-	-
5d	$CHCl_3$	355 (3.64)	-[e]	-	-	-	-	-
14a	$CHCl_3$	395 (4.02)	523 (396)	6196	0.32	5.90	0.54	1.15
14a	C_6H_{14}	403 (3.73)	512 (356)	5283	0.29	5.43	0.53	1.31
14a	PhMe	398 (3.97)	517 (398)	5783	0.37	5.71	0.65	1.10
14a	THF	392 (4.00)	523 (392)	6390	0.24	5.36	0.45	1.42
14a	MeCN	385 (4.02)	533 (385)	7212	0.13	3.56	0.36	2.44
14a	MeOH	-[f]	-	-	-	-	-	-
14b	$CHCl_3$	417 (4.06)	543 (417)	5565	0.28	2.03	1.38	3.55
14b	PhMe	417 (4.10)	534 (417)	5254	0.11	1.89	0.58	4.71
14c	$CHCl_3$	385 (3.97)	521 (387)	6780	0.24	4.99	0.48	1.52
14c	PhMe	387 (3.98)	515 (392)	6422	0.28	4.59	0.61	1.57
14d	$CHCl_3$	399 (3.92)	530 (399)	6195	0.18	4.57	0.39	1.79
14d	PhMe	395 (3.97)	522 (395)	6159	0.26	4.80	0.54	1.54
16	$CHCl_3$	392 (4.34)	411, 432 (373)	1179	0.12	0.53	2.26	16.6
17	$CHCl_3$	433 (4.44)	-[e]	-	-	-	-	-
18	$CHCl_3$	464 (4.45)	555 (464)	3534	0.15	2.03	0.74	4.19
18	PhMe	462 (4.50)	537 (422)	3023	0.20	1.81	1.10	4.42

[a] Measured at room temperature. [b] Determined by the absolute method. [c] Radiative rate constant k_f is calculated as $k_f = \Phi/T$. [d] Non-radiative rate constant k_{nr} is calculated as $k_{nr} = (1-\Phi)/T$. [e] Non fluorescent. [f] Not stable in Methanol.

Optical Properties in Solution and Solid State

Since the synthesized compounds contain different aromatic backbones and show structural differences in the solid state, they were investigated by UV/Vis and emission spectroscopy. A comparison of compounds with the same backbone (e.g. thienoquinolines **4a**, **5a** and **14a**) shows a significant change in optical properties depending on the substituent in 2'-position (Figure 6A and Table 4) in chloroform solutions. A methoxy substituent in this position, as present in molecule **5a** prevents the co-planarization of the aromatic systems (comparable to the observations in solid state as discussed above) leading to the most redshifted absorption at λ_{abs} = 339 nm. For the phenol analogue **4a** the most redshifted maximum is bathochromically

10.1002/chem.201604421

shifted about $\Delta\lambda$ = +25 nm to λ_{max} = 364 nm, which can be explained with a higher co-planarity of the two aryl systems as a result of the intramolecular cyclic hydrogen bond.[33] Upon the introduction of the BF_2-centers another bathochromical shift of $\Delta\lambda$ = +31 nm to λ_{abs} = 395 nm is observed for complex **14a**. Similar trends exist for all investigated series (see Table 4 and Supporting Information) and are not further discussed in detail. The most extended systems (**16-18**) show absorptions between λ_{abs} = 392 nm (**16**) and λ_{abs} = 462 nm (complex **18**) (Table 4). A comparison of the five boroquinols (Figure 6B) reveal that the three complexes with three annulated rings (**14a**, **14c** and **14d**) have comparable low energy absorption bands with maxima between λ_{abs} = 385 nm (**14c**) and λ_{abs} = 399 nm (**14d**). Complex **14b** with four annulated rings has its most redshifted absorption maximum at λ_{abs} = 417 nm and the extended bis-complex **18** at λ_{abs} = 464 nm (Figure 6B and Table 4). In contrast to negligible emissions of some of the precursors (**5b** and **16**), boroquinols **14a-d** and **18** show emission in chloroform solution with maxima between λ_{em} = 521 nm (**14c**) and λ_{em} = 555 nm (**18**) (Figure 6C and Table 4) and quantum yields between Φ = 0.15 (**18**) and Φ = 0.32 (**14a**). Other boranils and smaller boroquinols had to be decorated with electron donating or electron donating and accepting groups (push-pull systems) to emit at comparable wavelenghts (boranils: λ_{em} = 445-539 nm),[11] whereas for example unsubstituted smaller boroquinols emit at λ_{em} = 476 nm.[7b]

The emission properties of boroquinol **14a** were extensively investigated in various solvents (Table 4 and Supporting Information) and show an increasing quantum yield with decreasing solvent polarity ranging from Φ = 0.13 in acetonitrile to Φ = 0.37 in toluene. Interestingly, the quantum yield in hexane (Φ = 0.29) is rather low considering the non-polar character of the solvent. This and the lower extinction coefficient compared to other solvents (see Table 4) could be attributed to the low solubility in hexane accompanied by formation of aggregates. In methanol a deborylation was observed (see Supporting Information), which is in agreement to observations made before for other boroquinols.[7b] Complex **14b** exhibits a quantum yield of Φ = 0.28 in chloroform and is within this series the only complex showing a lower quantum yield in toluene (Φ = 0.11) in comparison to chloroform. The boroquinols with methoxy substituted phenanthridine backbones (**14c** and **14d**) show comparable quantum yields of Φ = 0.24 (**14c**) and Φ = 0.18 (**14d**) in chloroform and 0.04-0.06 higher quantum yield in toluene (see Table 4).

The fluorescence lifetimes of the complexes with three annulated rings (**14a**, **14c** and **14d**) are with τ = 4.57-5.90 ns significantly higher than the ones of complexes **14b** or **18** (τ = 2.03 ns) (Table 4). The resulting radiative rate constants increase for all boroquinols from chloroform to toluene (Table 4); again with **14b** as only exception. The difference in the decrease of the radiative rate constant k_f in comparison to the non-radiative rate constant k_{nr} (Table 4) shows that the lower quantum yields of **14d** and **18** are more likely to be attributed to an increase of non-radiative processes than to a destabilization of the corresponding excited states.

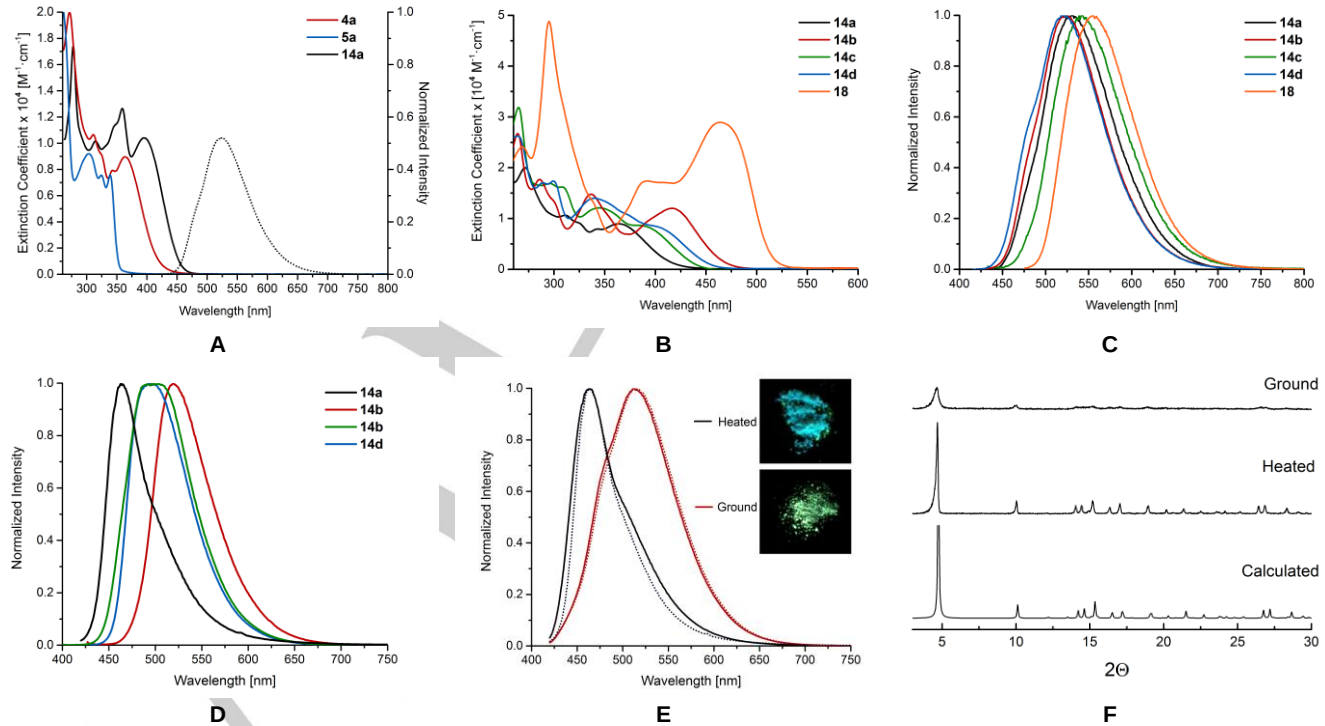

Figure 6. A: UV/Vis spectra of compounds **4a**, **5a** and **14a** and emission spectrum of **14a** in $CHCl_3$ at room temperature. B: UV/Vis spectra of complexes **14a-d** and **18** in $CHCl_3$ at room temperature. C: Emission spectra of complexes **14a-d** and **18** in $CHCl_3$ at room temperature. D: Emission spectra of complexes **14a-d** in solid state at room temperature. E: Emission spectra of complexes **14a** in solid state heated (T = 200 °C) and ground. The dashed lines display a second circle of heating and grinding. The inlet shows photographs of the solid materials irradiated at λ = 366 nm. F: PXRD patterns of **14a**: top: mechanically ground material; middle: heated material; calculated from single crystal x-ray analysis.

In comparison to the emissions in solution ($CHCl_3$), the emissions in solid state (Figure 6C, 6D and 6E, Tables 4 and 5) are hypsochromically shifted for the as-synthesized solid materials. For **14a** a large shift of $\Delta\lambda$ = -59 nm ($\lambda_{em\ solution}$ = 523 nm; $\lambda_{em\ solid}$ = 464 nm) has been observed. Most interestingly, boroquinols **14a** and **14d** show a mechanochromic behaviour[34] in the solid upon mechanical grinding of the as-synthesized solids.

Table 5. Emission spectroscopy data of complexes **14a-d** in solution and solid state.

Cmp #	λ_{em} ($CHCl_3$) [nm]	λ_{em} (solid) [nm][a]	λ_{em} (solid) [nm][b]
14a	523	464	514
14b	543	519	524
14c	521	510	511
14d	530	495	524

[a] As-synthesized solid material. [b] Mechanically ground solid material.

Again **14a** shows the largest shift of $\Delta\lambda$ = +50 nm ($\lambda_{em,\ as\text{-}synthesized}$ = 464 nm; $\lambda_{em\ ground}$ = 514 nm; Table 5, Figure 6E), which was fully reversible upon heating (T = 200 °C). In general a change in morphology of the fluorescent solid material has been pointed out to be the reason for mechanochromic effects.[35] Boroquinol **14a** was investigated by powder x-ray diffraction (PXRD) to get further insight to the origin of the observed effects. The as-synthesized material has a high degree of crystallinity, which is largely decreased upon grinding (Figure 6F). The reason for the change in emission wavelength could be explained with the presence of strong intermolecular interactions such as π-π-interactions in the ordered (or as-synthesized) phase, as seen in the X-ray crystal structure (as discussed above, Figure 4A-B). Since the measured PXRD-pattern fits perfectly to one calculated from the crystal structure, it can be concluded that these interactions elucidated by single crystal x-ray analysis are also present in the as-synthesized crystalline material. The shear forces applied by the mechanical stimulus is potentially changing the intermolecular interactions on a molecular level and therefore the degree of crystallinity. The resulting meta-stable state and its accompanied intermolecular interactions allow different transitions upon excitation and cause the observed change of the emission wavelength. The shift of the emission wavelength can be also seen by pure eye as the colour changes from light blue (as-synthesized or heated) to yellow (ground) as depicted in the inlet of Figure 6E.

The thermal reversibility of the obtained effects was proven by subsequent heating and grinding of the solid material. Solid state fluorescence spectroscopy proved the complete reversibility of both, the emissions maxima and the shape of the emission bands (Figure 6E). The reversibility can best be explained by reorganisation of the metastable amorphous state by lattice vibration upon heating and crystallization.[35a]

A similar mechanochromic effect was observed for **14d,** which shows a bathochromic shift of $\Delta\lambda$ =+28 nm upon grinding (Table 5 and Supporting Information). However, the thermal reversibility of **14d** was not investigated, because it decomposes at rather low temperatures (T > 60 °C).

Complexes **14b** and **14c** only show negligible changes of their emission wavelength upon grinding (Table 5 and Supporting Information).

DFT Calculations

To obtain more detailed information about the influence of the π-extension of the backbones of boroquinols **14a-d** and **18** the relative energy levels of frontier molecular orbitals have been calculated at the B3LYP/6-311+G** level of theory.[36]

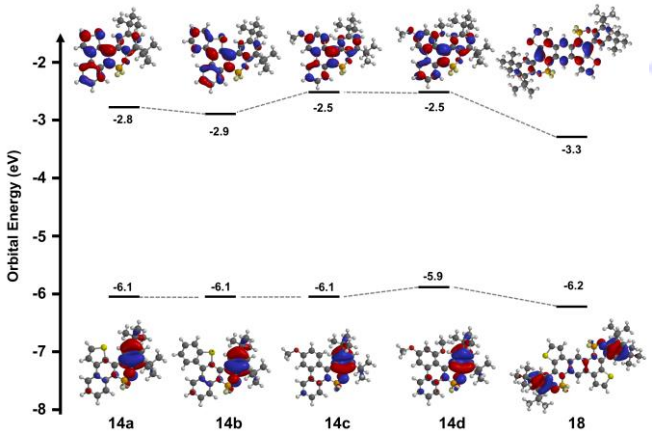

Figure 7. DFT calculations of frontier molecular orbitals and energy levels at the B3LYP/6-311+G** level of theory of boroquinols **14a-d** and **18**.

The calculated energy levels of the HOMOs of all five complexes (Figure 7) are with E_{HOMO} = -6.2 eV (**18**) to E_{HOMO} = -5.9 eV (**14d**) in a similar range. In all cases, the largest orbital coefficients of the HOMO are localized on the former salicylaldehyde part, which is the same for all compounds. The largest orbital coefficients of the LUMOs can be found on the extended aromatic backbone. Electron donating methoxy groups, as found in **14c** and **14d** increase the energies of the LUMOs to E_{LUMO} = -2.5 eV in both cases, indicating that the influence of the methoxy group in 7-position is negligible. **14a** (E_{LUMO} = -2.8 eV) and **14b** (E_{LUMO} = -2.9 eV) show comparable LUMO energies resulting in HOMO-LUMO differences of $\Delta(E_{LUMO}\text{-}E_{HOMO})$ = 3.2-3.3 eV. The LUMO of complex **18** was found at E_{LUMO} = -3.3 eV and the resulting HOMO-LUMO difference of $\Delta(E_{LUMO}\text{-}E_{HOMO})$ = 2.9 eV is the smallest for all five complexes. This is reflected by the most redshifted absorption and emission as discussed above.

Conclusions

We successfully applied the Pictet-Spengler reaction to synthesize π-extended ligands with *N,O*-chelating moieties. During the synthesis a barely described side-reaction was found and a plausible mechanism suggested by evaluation of various

screening conditions. According to the suggested mechanism, the conditions have finally been optimized, giving the ligands for the boroquinols in high yields. The corresponding fluorescent boroquinols emitted at wavelengths up to λ_{em} = 555 nm with quantum yields up to Φ = 0.37. Remarkably, some complexes showed large Stokes shifts (>7200 cm^{-1}) or a mechanochromic behavior in solid state by a transition between amorphous and crystalline phases, which has been proved by PXRD. As has been demonstrated with the larger compound with a heteropicene-based backbone, the optimized reaction conditions opens the possibility to larger structures containing more than one BF_2-unit and opens the possibility to be applied for typical products by dynamic covalent chemistry contain salicyl imines, such as macrocycles[37] or cage compounds,[38] which is currently investigated in our laboratories.

Experimental Section

All crystallographic information files (CCDC-1503734 [**4a**], 1503735 [**4b**], 1503736 [**4c**], 1503737 [**4d**], 1503738 [**5a**], 1503739 [**5b**], 1503740 [**5c**], 1503741 [**5d**], 1503742 [**14a**], 1503743 [**14b**], 1503744 [**14c**], 1503745 [**14d**], 1503742 [**16**], 1503742 [**17**] and 1503742 [**18**]) have been deposited in the Cambridge Crystallographic Data Centre and can be downloaded free of charge via www.ccdc.camac.uk/data_request/cif.ls.

Supporting Information (see footnote on the first page of this article): For synthetic procedures, characterization and spectra of the discussed molecules see Supporting Information.

Acknowledgements

S. M. E. is grateful to the *Studienstiftung des deutschen Volkes* for a PhD scholarship. Hendrik Herrmann (Himmel Group) and Petra Krämer (Hashmi Group) are acknowledged for PXRD and IR measurements.

Keywords: fluorescence • boron complexes • extended π-system • mechanochromism • Pictet-Spengler reaction

[1] For reviews see: a) A. Loudet and K. Burgess, *Chem. Rev.* **2007**, *107*, 4891-4932; b) R. Ziessel, G. Ulrich and A. Harriman, *New J. Chem.* **2007**, *31*, 496-501; c) G. Ulrich, R. Ziessel and A. Harriman, *Angew. Chem. Int. Ed.* **2008**, *47*, 1184-1201; d) N. Boens, V. Leen and W. Dehaen, *Chem. Soc. Rev.* **2012**, *41*, 1130-1172; e) D. Frath, J. Massue, G. Ulrich and R. Ziessel, *Angew. Chem. Int. Ed.* **2014**, *53*, 2290-2310; f) A. Kamkaew, S. H. Lim, H. B. Lee, L. V. Kiew, L. Y. Chung and K. Burgess, *Chem. Soc. Rev.* **2013**, *42*, 77-88.

[2] a) M. Baruah, W. Qin, N. Basarić, W. M. De Borggraeve and N. Boens, *J. Org. Chem.* **2005**, *70*, 4152-4157; b) M. Benstead, G. H. Mehl and R. W. Boyle, *Tetrahedron* **2011**, *67*, 3573-3601.

[3] a) J. Chen, A. Burghart, A. Derecskei-Kovacs and K. Burgess, *J. Org. Chem.* **2000**, *65*, 2900-2906; b) H. Lu, J. Mack, Y. Yang and Z. Shen, *Chem. Soc. Rev.* **2014**, *43*, 4778-4823.

[4] For recent examples of BODIPY derivatives see: a) J. Bartelmess, M. Baldrighi, V. Nardone, E. Parisini, D. Buck, L. Echegoyen and S. Giordani, *Chem. Eur. J.* **2015**, *21*, 9727-9732; b) B. Basumatary, A. Raja Sekhar, R. V. Ramana Reddy and J. Sankar, *Inorg. Chem.* **2015**, *54*, 4257-4267; c) B. Basumatary, R. V. Ramana Reddy, S. Bhandary and J. Sankar, *Dalton Trans.* **2015**, *44*, 20817-20821; d) C. Caltagirone, M. Arca, A. M. Falchi, V. Lippolis, V. Meli, M. Monduzzi, T. Nylander, A. Rosa, J. Schmidt, Y. Talmon and S. Murgia, *RSC Adv.* **2015**, *5*, 23443-23449; e) J. H. Gibbs, H. Wang, N. V. S. D. K. Bhupathiraju, F. R. Fronczek, K. M. Smith and M. G. H. Vicente, *J. Organomet. Chem.* **2015**, *798, Part 1*, 209-213; f) L. A. Juárez, A. Barba-Bon, A. M. Costero, R. Martínez-Máñez, F. Sancenón, M. Parra, P. Gaviña, M. C. Terencio and M. J. Alcaraz, *Chem. Eur. J.* **2015**, *21*, 15486-15490; g) S. Knippenberg, M. V. Bohnwagner, P. H. P. Harbach and A. Dreuw, *J. Phys. Chem. A* **2015**, *119*, 1323-1331; h) A. N. Kursunlu, *Tetrahedron Lett.* **2015**, *56*, 1873-1877; i) M. Malachowska-Ugarte, C. Sperduto, Y. V. Ermolovich, A. L. Sauchuk, M. Jurášek, R. P. Litvinovskaya D. Straltsova, I. Smolich, V. N. Zhabinskii, P. Drašar, V. Demidchik and V. A. Khripach, *Steroids* **2015**, *102*, 53-59; j) N. I. Shlyakhtina, A. V. Safronov, Y. V. Sevryugina, S. S. Jalisatgi and M. F. Hawthorne, *J. Organomet. Chem* **2015**, *798, Part 1*, 234-244; k) T. Sun, X. Guan, M. Zheng, X. Jing and Z. Xie, *ACS Med. Chem. Lett.* **2015**, *6*, 430-433; l) M. R. Topka and P. H. Dinolfo, *ACS Appl. Mater. Interfaces* **2015**, *7*, 8053-8060; m) M. Ucuncu, E. Karakus and M. Emrullahoglu, *New J. Chem.* **2015**, *39*, 8337-8341; n) F. Wang, Y. Zhu, L. Zhou, L. Pan, Z. Cui, Q. Fei, S. Luo, D. Pan, Q. Huang, R. Wang, C. Zhao, H. Tian and C. Fan, *Angew. Chem. Int. Ed.* **2015**, *54*, 7349-7353; o) Z.-X. Zhang, X.-F. Guo, H. Wang and H.-S. Zhang, *Anal. Chem.* **2015**, *87*, 3989-3995; p) N. Zhao, S. Xuan, F. R. Fronczek, K. M. Smith and M. G. H. Vicente, *J. Org. Chem.* **2015**, *80*, 8377-8383.

[5] For recent examples see: a) S. M. Barbon, V. N. Staroverov and J. B. Gilroy, *J. Org. Chem.* **2015**, *80*, 5226-5235; b) Y. Fu, F. Qiu, F. Zhang, Y. Mai, Y. Wang, S. Fu, R. Tang, X. Zhuang and X. Feng, *Chem. Commun.* **2015**, *51*, 5298-5301; c) C. Glotzbach, N. Godeke, R. Frohlich, C.-G. Daniliuc, S. Saito, S. Yamaguchi and E.-U. Wurthwein, *Dalton Trans.* **2015**, *44*, 9659-9671; d) Q. Lin, S. Xiao, R. Li, R. Tan, S. Wang and R. Zhang, *Dyes Pigm.* **2015**, *114*, 33-39; e) Q. Liu, X. Wang, H. Yan, Y. Wu, Z. Li, S. Gong, P. Liu and Z. Liu, *J. Mater. Chem. C* **2015**, *3*, 2953-2959; f) R. R. Maar, S. M. Barbon, N. Sharma, H. Groom, L. G. Luyt and J. B. Gilroy, *Chem. Eur. J.* **2015**, *21*, 15589-15599; g) Y. Meesala, V. Kavala, H.-C. Chang, T.-S. Kuo, C.-F. Yao and W.-Z. Lee, *Dalton Trans.* **2015**, *44*, 1120-1129; h) D. Suresh, C. S. B. Gomes, P. S. Lopes, C. A. Figueira, B. Ferreira, P. T. Gomes, R. E. Di Paolo, A. L. Maçanita, M. T. Duarte, A. Charas, J. Morgado, D. Vila-Viçosa and M. J. Calhorda, *Chem. Eur. J.* **2015**, *21*, 9133-9149; i) Y. Wu, H. Lu, S. Wang, Z. Li and Z. Shen, *J. Mater. Chem. C* **2015**, *3*, 12281-12289; j) C. Yu, E. Hao, T. Li, J. Wang, W. Sheng, Y. Wei, X. Mu and L. Jiao, *Dalton Trans.* **2015**, *44*, 13897-13905; k) Q. Liu, C. Zhang, X. Wang, S. Gong, W. He and Z. Liu, *Chem. Asian J.* **2016**, *11*, 202-206; l) T. Nakamura, S. Furukawa and E. Nakamura, *Chem. Asian J.* **2016**, *11*, 2016-2020; m) T. M. H. Vuong, J. Weimmerskirch-Aubatin, J.-F. Lohier, N. Bar, S. Boudin, C. Labbe, F. Gourbilleau, H. Nguyen, T. T. Dang and D. Villemin, *New J. Chem.* **2016**, *40*, 6070-6076; n) S. Wang, R. Tan, Y. Li, Q. Li and S. Xiao, *Dyes Pigm.* **2016**, *132*, 342-346.

[6] For recent examples see: a) A. D'Aleo, F. Abdellah and F. Frédéric, *Adv. Nat. Sci.: Nanosci. Nanotechnol.* **2015**, *6*, 015009; b) S. Guieu, J. Pinto, V. L. M. Silva, J. Rocha and A. M. S. Silva, *Eur. J. Org. Chem.* **2015**, *2015*, 3423-3426; c) P.-H. Lanoë, B. Mettra, Y. Y. Liao, N. Calin, A. D'Aléo, T. Namikawa, K. Kamada, F. Fages, C. Monnereau and C. Andraud, *ChemPhysChem* **2016**, *17*, 2128-2136; d) S. Mo, C. Xu and J. Xu, *Adv. Synth. Catal.* **2016**, *358*, 1767-1777.

[7] For recent examples see: a) S. Hachiya, D. Hashizume, H. Ikeda, M. Yamaji, S. Maki, H. Niwa and T. Hirano, *J. Photochem. Photobiol., A*; b) U. Balijapalli and S. K. Iyer, *Eur. J. Org. Chem.* **2015**, *2015*, 5089-5098; c) G. G. Dias, B. L. Rodrigues, J. M. Resende, H. D. R. Calado, C. A. de Simone, V. H. C. Silva, B. A. D. Neto, M. O. F. Goulart, F. R. Ferreira, A. S. Meira, C. Pessoa, J. R. Correa and E. N. da Silva Junior, *Chem. Commun.* **2015**, *51*, 9141-9144; d) L. Fan, L. Wu and M. Ke, *J. Chem. Res.* **2015**, *39*, 442-

444; e) A. Kilic, F. Alcay, M. Aydemir, M. Durgun, A. Keles and A. Baysal, *Spectrochim. Acta, Part A* **2015**, *142*, 62-72; f) Y. Kubota, K. Kasatani, H. Takai, K. Funabiki and M. Matsui, *Dalton Trans.* **2015**, *44*, 3326-3341; g) H. S. Kumbhar, B. L. Gadilohar and G. S. Shankarling, *Spectrochim. Acta, Part A* **2015**, *146*, 80-87; h) H. S. Kumbhar and G. S. Shankarling, *Dyes Pigm.* **2015**, *122*, 85-93; i) C.-W. Liao, R. Rao M and S.-S. Sun, *Chem. Commun.* **2015**, *51*, 2656-2659; j) E. V. Nosova, T. N. Moshkina, G. N. Lipunova, I. V. Baklanova, P. A. Slepukhin and V. N. Charushin, *J. Fluorine Chem.* **2015**, *175*, 145-151; k) D.-E. Wu, X.-L. Lu and M. Xia, *New J. Chem.* **2015**, *39*, 6465-6473; l) G. F. Wu, Q. L. Xu, L. E. Guo, T. N. Zang, R. Tan, S. T. Tao, J. F. Ji, R. T. Hao, J. F. Zhang and Y. Zhou, *Tetrahedron Lett.* **2015**, *56*, 5034-5038; m) Z. Zhang, Z. Wu, J. Sun, B. Yao, G. Zhang, P. Xue and R. Lu, *J. Mater. Chem. C* **2015**, *3*, 4921-4932; n) J. Zheng, F. Huang, Y. Li, T. Xu, H. Xu, J. Jia, Q. Ye and J. Gao, *Dyes Pigm.* **2015**, *113*, 502-509; o) J. Zheng, Y. Li, Y. Cui, J. Jia, Q. Ye, L. Han and J. Gao, *Tetrahedron* **2015**, *71*, 3802-3809; p) K. Benelhadj, J. Massue and G. Ulrich, *New J. Chem.* **2016**, *40*, 5877-5884.

[8] D. Frath, S. Azizi, G. Ulrich and R. Ziessel, *Org. Lett.* **2012**, *14*, 4774-4777.

[9] J. F. Chandler, B. Dobinson, E. Johnston, M. E. B. Jones, R. J. Martin and B. P. Stark, *Br. Polym. J.* **1969**, *1*, 208-212.

[10] F. Umland, E. Hohaus and K. Brodte, *Chem. Ber.* **1973**, *106*, 2427-2437.

[11] D. Frath, S. Azizi, G. Ulrich, P. Retailleau and R. Ziessel, *Org. Lett.* **2011**, *13*, 3414-3417.

[12] R.-Z. Ma, Q.-C. Yao, X. Yang and M. Xia, *J. Fluorine Chem.* **2012**, *137*, 93-98.

[13] J. H. Burroughes, D. D. C. Bradley, A. R. Brown, R. N. Marks, K. Mackay, R. H. Friend, P. L. Burns and A. B. Holmes, *Nature* **1990**, *347*, 539-541.

[14] X. Yang and M. Xia, *Acta Crystallogr., Sect. E: Struct. Rep. Online* **2011**, *67*, o1049.

[15] a) J. Feng, B. Liang, D. Wang, L. Xue and X. Li, *Org. Lett.* **2008**, *10*, 4437-4440; b) Y. Zhou, Y. Xiao, S. Chi and X. Qian, *Org. Lett.* **2008**, *10*, 633-636; c) M.-X. Zhang, S. Chai and G.-J. Zhao, *Org. Electron.* **2012**, *13*, 215-221.

[16] A. Pictet and T. Spengler, *Ber. Dtsch. Chem. Ges.* **1911**, *44*, 2030-2036.

[17] a) A. K. Mandadapu, M. Saifuddin, P. K. Agarwal and B. Kundu, *Org. Biomol. Chem.* **2009**, *7*, 2796-2803; b) S. W. Youn and J. H. Bihn, *Tetrahedron Lett.* **2009**, *50*, 4598-4601.

[18] a) M. Akula, J. P. Sridevi, P. Yogeeswari, D. Sriram and A. Bhattacharya, *Monatsh. Chem.* **2014**, *145*, 811-819; b) M. Akula, Y. Thigulla, C. Davis, M. Jha and A. Bhattacharya, *Org. Biomol. Chem.* **2015**, *13*, 2600-2605; c) M. Akula, Y. Thigulla, A. Nag and A. Bhattacharya, *RSC Adv.* **2015**, *5*, 74539-74540; d) M. Akula, Y. Thigulla, A. Nag and A. Bhattacharya, *RSC Adv.* **2015**, *5*, 57231-57234.

[19] M. Tasior, M. Chotkowski and D. T. Gryko, *Org. Lett.* **2015**, *17*, 6106-6109.

[20] T. Chatterjee, M. G. Choi, J. Kim, S.-K. Chang and E. J. Cho, *Chem. Commun.* **2016**, *52*, 4203-4206.

[21] J. Tummatorn, S. Krajangsri, K. Norseeda, C. Thongsornkleeb and S. Ruchirawat, *Org. Biomol. Chem.* **2014**, *12*, 5077-5081.

[22] B. Berionni Berna, S. Nardis, P. Galloni, A. Savoldelli, M. Stefanelli, F. R. Fronczek, K. M. Smith and R. Paolesse, *Org. Lett.* **2016**, *18*, 3318-3321.

[23] J. K. Augustine, A. Bombrun, P. Alagarsamy and A. Jothi, *Tetrahedron Lett.* **2012**, *53*, 6280-6287.

[24] Y. Zhu, H. Zhao and Y. Wei, *Synthesis* **2013**, *45*, 952-958.

[25] a) M. S. Carpenter, W. M. Easter and T. F. Wood, *J. Org. Chem.* **1951**, *16*, 586-617; b) A. V. Nizovtsev, A. Scheurer, B. Kosog, F. W. Heinemann and K. Meyer, *Eur. J. Inorg. Chem.* **2013**, *2013*, 2538-2548.

[26] N. Miyaura and A. Suzuki, *Chem. Rev.* **1995**, *95*, 2457-2483.

[27] a) D. G. Lloyd, R. B. Hughes, D. M. Zisterer, D. C. Williams, C. Fattorusso, B. Catalanotti, G. Campiani and M. J. Meegan, *J. Med. Chem.* **2004**, *47*, 5612-5615; b) M. Roberti, D. Pizzirani, M. Recanatini, D. Simoni, S. Grimaudo, C. Di, V. Abbadessa, N. Gebbia and M. Tolomeo, *J. Med. Chem.* **2006**, *49*, 3012-3018.

[28] B. J. Stokes, B. Jovanović, H. Dong, K. J. Richert, R. D. Riell and T. G. Driver, *J. Org. Chem.* **2009**, *74*, 3225-3228.

[29] A. S. Zektzer, M. J. Quast, G. S. Linz, G. E. Martin, J. D. McKenney, M. D. Johnston and R. N. Castle, *Magn. Reson. Chem.* **1986**, *24*, 1083-1088.

[30] a) M. Domagała, S. J. Grabowski, K. Urbaniak and G. Mlostoń, *J. Phys. Chem. A* **2003**, *107*, 2730-2736; b) M. Domagała and S. J. Grabowski, *J. Phys. Chem. A* **2005**, *109*, 5683-5688.

[31] V. R. Thalladi, H.-C. Weiss, D. Bläser, R. Boese, A. Nangia and G. R. Desiraju, *J. Am. Chem. Soc.* **1998**, *120*, 8702-8710.

[32] a) F. B. Mallory, C. W. Mallory and W. M. Ricker, *J. Org. Chem.* **1985**, *50*, 457-461; b) S. C. F. Kui, N. Zhu and M. C. W. Chan, *Angew. Chem. Int. Ed.* **2003**, *42*, 1628-1632.

[33] G. Gilli, F. Bellucci, V. Ferretti and V. Bertolasi, *J. Am. Chem. Soc.* **1989**, *111*, 1023-1028.

[34] Y. Sagara and T. Kato, *Nat. Chem.* **2009**, *1*, 605-610.

[35] a) Z. V. Todres, *J. Chem. Res.* **2004**, *2004*, 89-93; b) G. Zhang, J. Lu, M. Sabat and C. L. Fraser, *J. Am. Chem. Soc.* **2010**, *132*, 2160-2162.

[36] a) A. D. Becke, *Phys. Rev. A* **1988**, *38*, 3098-3100; b) C. Lee, W. Yang and R. G. Parr, *Phys. Rev. B* **1988**, *37*, 785-789.

[37] For examples of suitable systems see: a) S. Akine, T. Taniguchi and T. Nabeshima, *Tetrahedron Lett.* **2001**, *42*, 8861-8864; b) S. Akine, D. Hashimoto, T. Saiki and T. Nabeshima, *Tetrahedron Lett.* **2004**, *45*, 4225-4227; c) A. J. Gallant, J. K. H. Hui, F. E. Zahariev, Y. A. Wang and M. J. MacLachlan, *J. Org. Chem.* **2005**, *70*, 7936-7946; d) A. J. Gallant, M. Yun, M. Sauer, C. S. Yeung and M. J. MacLachlan, *Org. Lett.* **2005**, *7*, 4827-4830; e) J. K. H. Hui and M. J. MacLachlan, *Chem. Commun.* **2006**, 2480-2482; f) T. Nabeshima, H. Miyazaki, A. Iwasaki, S. Akine, T. Saiki and C. Ikeda, *Tetrahedron* **2007**, *63*, 3328-3333; g) B. N. Boden, J. K. H. Hui and M. J. MacLachlan, *J. Org. Chem.* **2008**, *73*, 8069-8072; h) P. D. Frischmann J. Jiang, J. K. H. Hui, J. J. Grzybowski and M. J. MacLachlan, *Org. Lett.* **2008**, *10*, 1255-1258; i) K. E. Shopsowitz, D. Edwards, A. J. Gallant and M. J. MacLachlan, *Tetrahedron* **2009**, *65*, 8113-8119; j) S. Akine, F. Utsuno and T. Nabeshima, *Chem. Commun.* **2010**, *46*, 1029-1031; k) S. Guieu, A. K. Crane and M. J. MacLachlan, *Chem. Commun.* **2011**, *47*, 1169-1171; l) M. Yamamura, H. Miyazaki, M. Iida, S. Akine and T. Nabeshima, *Inorg. Chem.* **2011**, *50*, 5315-5317; m) J. K. H. Hui, J. Jiang and M. J. MacLachlan *Can. J. Chem.* **2012**, *90*, 1056-1062; n) S. Akine, S. Piao, M. Miyashita and T. Nabeshima, *Tetrahedron Lett.* **2013**, *54*, 6541-6544; o) S. Akine, M. Miyashita, S. Piao and T. Nabeshima, *Inorg. Chem. Front.* **2014**, *1*, 53-57.

[38] For examples of suitable systems see: a) Y. Liu, X. Liu and R. Warmuth, *Chem. Eur. J.* **2007**, *13*, 8953-8959; b) D. Xu and R. Warmuth, *J. Am. Chem Soc.* **2008**, *130*, 7520-7521; c) M. Mastalerz, M. W. Schneider, I. M. Oppel and O. Presly, *Angew. Chem.* **2011**, *123*, 1078-1083; d) M. W. Schneider, I. M. Oppel, H. Ott, L. G. Lechner, H.-J. S. Hauswald, R. Stoll and M. Mastalerz, *Chem. Eur. J.* **2012**, *18*, 836-847; e) M. W. Schneider, H.-J. Siegfried Hauswald, R. Stoll and M. Mastalerz, *Chem. Commun.* **2012**, *48*, 9861-9863; f) S. M. Elbert, F. Rominger and M. Mastalerz, *Chem. Eur. J.* **2014**, *20*, 16707-16720.

10.1002/chem.201604421

WILEY-VCH

Entry for the Table of Contents (Please choose one layout)

Layout 1:

FULL PAPER

Stiff it up. By Pictet-Spengler cyclisations a series of boroquinols with extended π-backbones have been made accessible. Some of them showing reversible mechanochromical effects upon grinding. During the Pictet-Spengler cyclization a rarely described fragmentation under C-C-bond cleavage occurred, for which s plausible mechanism could be suggested on the basis of various reaction conditions.

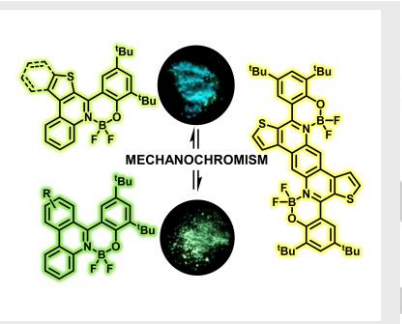

*Sven M. Elbert, Philippe Wagner, Thines Kanagasundaram, Frank Rominger and Michael Mastalerz**

Page No. – Page No.

Boroquinol Complexes with fused Extended Aromatic Backbones – Synthesis and Optical Properties